Study and Analysis of a Remote Robot-assisted Ultrasound Imaging System

Chuan Geng[1], Qiang xie[2*], Long Chen[2], Alex Li[2], Binjie Qin[1]
1. School of Biomedical Engineering, Shanghai Jiao Tong University, Shanghai, China
2. Wuhan United Imaging Healthcare Surgical Technology Co., Ltd, Wuhan, China
gengchuan@sjtu.edu.cn, qiang.xie@united-imaging.com, long.chen01@united-imaging.com, Alex.li@united-imaging.com, binjie.qin@qq.com

***Abstract*—Ultrasound(US) imaging is widely employed in diagnosing diseases because of its low cost, high efficiency and less harmfulness to patients. However, experienced doctors are required to operate the system and interpret ultrasound image. In this paper, a robot assisted ultrasound imaging system is developed for remote ultrasonic diagnosis, in which a master-slave mapping relationship is established based on velocity control of incremental position and orientation. Butterworth low-pass filtering is applied to suppress the jitter signal at the master side and improve the smoothness at the slave side. Finally, an ultrasound imaging experiment is carried out and the effectiveness and feasibility of remote robot-assisted ultrasound imaging system are verified.**

Keywords—master-slave, velocity control, robot-assisted ultrasound imaging, remote control

I. INTRODUCTION

The application of ultrasound imaging in medical diagnosis has been enormously growing over several decades. Because of its outstanding features such as non-radiation, real-time, portability, low cost, etc, ultrasound has become one of mainstream medical imaging equipment[1]. However, ultrasound imaging quality generally depends on the doctor's professional skills and experience in manipulating the system setting while handling the ultrasound probe[2]. Under many situations, a skilled sonographer may not be available especially in rural and remote areas. On the other hand, the longtime uncomfortable posture of the sonographer is likely to cause repetitive muscle damage during work. It is reported that 86% of cardiac sonographers suffer musculoskeletal pain[3]. Thus, the robot-assisted ultrasound imaging system has been studied to improve the quality and consistency of ultrasound imaging diagnosis, also reduce the workload of the sonographer in comparison with traditional ultrasound scans.

Based on the level of human-robot interaction, Monfaredi et al.[4] put the robot-assisted US imaging systems into three categories: autonomous robotic US imaging system, human-robot cooperated US imaging system and tele-operated US imaging system. The autonomous robotic US imaging systems are generally comprised of an ultrasound device, a robot arm and a tracking system. The tracking system can be optical tracking, electromagnetic tracking or passive encoded mechanical system [5~6]. The path of the ultrasound scan must be planned by the doctor in advance[7]. Human-robot cooperation system shares control degrees of freedom between the operator and the robot while this system is not capable for remote control. In remote robot-assisted ultrasound imaging, a master-slave architecture is commonly used for the remote control of the ultrasound probe. At master side, the sonographer uses the joystick or force feedback device to control the slave robot. The real-time ultrasound images are transferred and displayed on the monitor at the master side. By applying the force sensor fixed at the end of the robot, the operator can feel the force exerted on the human body through the force feedback system. It provides sufficient information to operator to adjust the direction and force applied to the ultrasound probe to capture the images that are required. Furthermore, new techniques such as deep learning can be applied to robotic ultrasound imaging for improving diagnostic accuracy and efficiency [8].

There are substantial amounts of feasibility studies conducted in remote robot-assisted ultrasound imaging in the past decades. Seo et al.[9] proposed a framework of the remote robot-assisted system and designed a new robot slave based on previous research in which 3D space mouse was set as master without force feedback. The system was able to acquire real-time ultrasound images remotely with good motion accuracy in x, y axis direction between master and slave sides. Fjellin et al.[10] implemented a master-slave control system. And the researchers designed experiments where using ultrasound to find a sphere inside a self-made phantom with and without force feedback. Results showed that volunteers could find the sphere more quickly with haptic feedback, which proved that it is necessary to achieve force feedback in master-slave system. Ju et al.[11] applied the position-to-position scheme to control the slave robot. The authors evaluated two control strategies: joint space and target space position-to-position control but no force/torque sensor was used in the study. Mathiassen et al.[12] described compliance force control and forward flow haptic control methods by using UR5 and Phantom Omni. But no clinical evaluation was performed.

In this paper, we construct a remote robot-assisted ultrasound imaging system by velocity control of the master-slave workspace. The structure is organized as follows: Section II describes the system architecture, system kinematical modeling, and the master-slave velocity mapping and control mechanism. Section III shows experimental results of the control mechanism along with real-time ultrasound imaging. Finally, summary and discussion of the proposed system are given in Section IV.

978-1-7281-4390-3/20/$31.00 ©2020 IEEE

II. The Material and Methods

A. The System Architecture

The proposed system as shown in Fig. 1 consists of the following parts: an US machine (Engineering prototype, China) with a convex array probe (CLA3.5, Vermon, France) for acquiring the B-scans image of phantom(Model 040GSE, Computerized Imaging Reference Systems, USA), a 6-DoF robotic arm (UR5, Universal Robots Corporation, Denmark), a haptic device (Touch, 3D System Corporation, America), a computer with an Intel Core i5-7400 and 8 GB RAM.

The Touch (serving as the master device which is controlled by the doctor and provides haptic feedback to the doctor) connects to the computer through USB connection. UR5 (serving as the slave device) and the computer are directly connected to a local area network with TCP/IP protocol of data transmission. An ultrasound probe is mounted on the end effector of UR5 by a clamp. Furthermore, the development environment is Visual Studio 2010 based on windows10 64bit system.

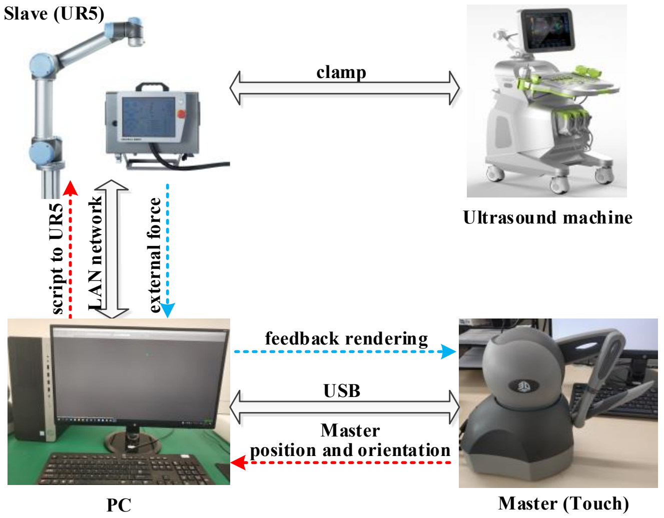

Fig. 1. Configuration and connection of the system and flow of information

B. The System Kinematical Modeling

Considering patient safety is extremely important for the reliable robot system, we choose the six joint cooperative robot UR5 from Universal Robots with the following considerations. On the one hand, UR5 complies with point 5.10.5 of the standard EN ISO 10218-1:2006 which means UR5 is credible in Human-Robot interaction, and on the other hand, the UR5 with 6 degrees of freedom(DOF)can reach an arbitrary position with at least one pose within a working radius of up to 33.5 ins (850mm). The standard Denavit–Hartenberg(DH)[13] model of UR5 and a calibrated parameters is provided by manufacturer. A handling gripper is designed to affixing the ultrasound probe on the distal end of the arm (Fig. 2).

As a programmable, economic haptic device, Touch has attracted many researchers' attention in the field of robot control[14]. Based on T Sansanayuth et al.'s effort[15], we summarize standard DH parameters as shown in Table I, where $l_1 = l_2 = 0.13335m$.

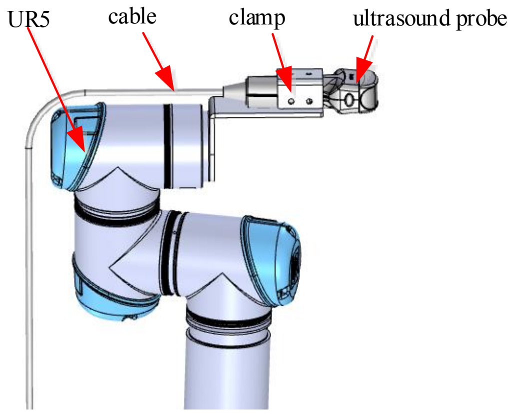

Fig. 2. Clamp is designed to hold probe .

TABLE I. DH Parameters of The Touch Device

Link i	θ_i (*angle* limit(deg))	d_i	a_i	α_i (*rad*)
1	$q_1(-56 \sim 56)$	0	0	-π/2
2	$q_2(0 \sim 100)$	0	l_1	0
3	$q_3(-47\sim69)$	0	0	-π/2
4	$q_4(-141\sim148)$	$-l_2$	0	π/2
5	$q_5(-87\sim57)\text{-}\pi/2$	0	0	π/2
6	$q_6(-150\sim150)\text{-}\pi/2$	0	0	π

C. The System Motion Control

In master-slave motion control, a control strategy is proposed as shown in Fig. 3. Mater's position p_m needs to be filtered and s represents a time derivation of p_m, and then Touch's final linear velocity v_m is calculated. k_v means scaling factor. Values of joint 1~6 $q_{1\sim6}$ are used for computing UR5's forward kinematic(FK). Then the computed rotation matrix Ts and Touch's joint 4~6 values $q_{4\sim6}$ are input to function F to calculate the needed angular velocity w_m. The contact force f between robot end effector and environment can be scaled by factor k_f and fed back to the master if a force sense is placed at

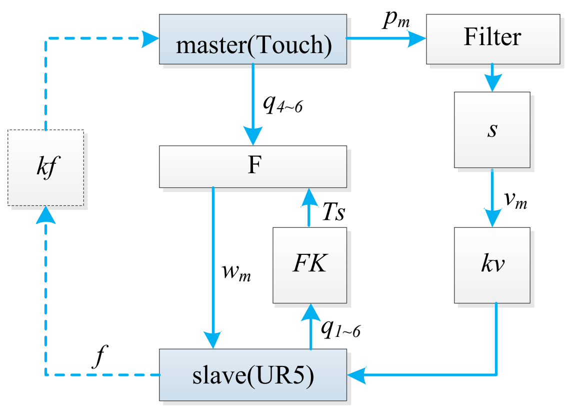

Fig. 3. Proposed master-slave motion control strategy

the end of the robot. Details will be descript in following paragraphs.

Generally, the information about a system tele-operated by a human operator is mainly distributed in the low frequency domain, whereas noises are in the high frequency part. C.J. Zandsteeg et al.[16] concluded that good position tracking up to 2Hz is necessary, while frequencies above 8Hz should be suppressed. In our work, a low-pass Butterworth filter with cutoff frequency 1Hz at -3dB of the pass band and cutoff frequency 5Hz at -25dB of the pass band was implemented. The properties of the low-pass filter as shown in Fig.3.

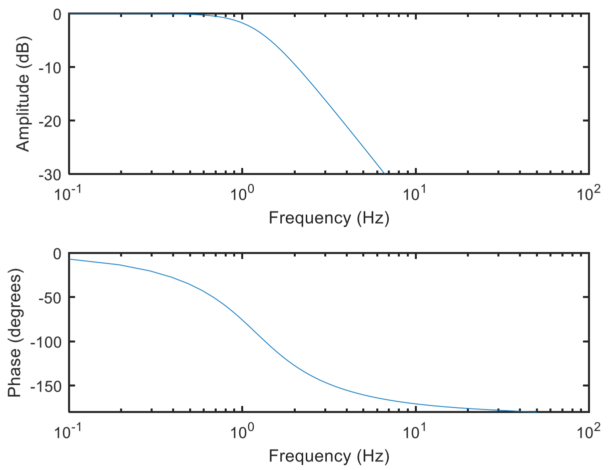

Fig. 4. Properties of implemented low-pass filter

In master-slave motion control, 100Hz of communication rates is regarded as good choice. The Touch updates frequency is 1000Hz. So 10 times down-sampling is needed to be realized. In consideration of internal controller of UR5, we cannot adopt some motion commands, such as 'movel', 'movep' and so on, in online real-time control. Because a new instruction cannot overwrite the former instruction which means there always has been a stop between two instructions. But command 'speedl' can overwrite the former command 'speedl' which means it is a good choice. UR5 scripts prescribe the form of sent 'speedl' as 'speedl(qd,a,t)' where $qd = [v_x, v_y, v_z, w_x, w_y, w_z]$, v is linear speed and w is angular speed relative to UR5 base, a is acceleration and t is running time. In realization, it is wise to consider the linear speed and the angular speed respectively.

In master-slave position control, only base coordinate transformation should be considered. We computed ${}^{s}T_m$ after kinematical modeling by the following equation.

$$ {}^{s}T_m = \begin{bmatrix} 0 & 0 & -1 \\ -1 & 0 & 0 \\ 0 & 1 & 0 \end{bmatrix} \quad (1) $$

Master linear speed $V_m = [v_x, v_y, v_z]^T$ can be read from API or computed by displacement difference and time. Then the speed part(v_s) of script would be sent to UR5 is $V_s = {}^{s}T_m \cdot V_m$.

In master-slave pose control, the master's pose is needed to be differentiated and the angular speed is got. We don't calculate Touch's attitude matrix by forward kinematic. We make linear relation between increment of the last three joint angles of Touch and the expected increment angles of UR5 rotating around x, y, z axis of UR5 base coordinate system. The wanted increment rotation matrix can be depicted as

$$ \Delta Rs = Rot(z, \Delta z) \times Rot(y, \Delta y) \times Rot(x, \Delta x) \quad (2) $$

Then target rotation matrix is calculated as

$$ Rs(t + \Delta t) = \Delta Rs \cdot Rs(t) \quad (3) $$

Through such a method, we can not only intuitively control UR5 through Touch, but also calculate angular velocity. Rotation matrix can be represented by quaternion and quaternion is easily to be differentiated. The derivatives of unit quaternion $Q(\mathrm{t})$ can be represented as

$$ Q'(\mathrm{t}) = 1/2 \cdot \omega(\mathrm{t}) \cdot Q(\mathrm{t}) \quad (4) $$

In formula (4), $\omega(\mathrm{t})$ is the angular velocity corresponding to $Q(\mathrm{t})$. In the discrete form, we can get

$$ Q[t + \Delta t] = Q[t] + \Delta t / 2 \cdot \Omega[t] \cdot Q[t] \quad (5) $$

In formula (5), $\Omega[\mathrm{t}]$ is the computed angular velocity of slave's pose. In this way, both position and pose should be sent to UR5 are computed.

III. EXPERIMENT

In order to assess the proposed master/slave system, we carry out a set of experiments. Three types of performances will be investigated through our experiments: jitter removal performance, translation velocity tracking and ultrasound imaging experiment.

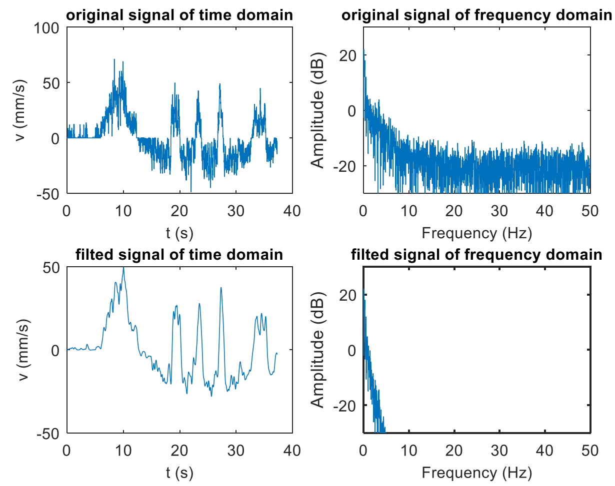

Fig. 5. Original and filted signal of time and frequency domains

It is not possible for a human holding the joystick to keep absolutely still over a long period of time. There can be some small movement of executor's hand at all time, which means there will be some small vibration random noise on the haptic device. In our random movement experiment, all of x, y, z axes noise exists and is presented as almost same waveform in frequency domain. To verify the effectiveness of filtering, we carry out the subjective random motion in the y-axis direction of the master hand. The results in time domain and frequency domain with and without filtering are shown in the Fig.5. The results shows that position control bandwidth is about 2Hz and filtered signal proves to be so consecutive that the shaking problem in the movement of robot is greatly suppressed.

In translation velocity tracking experiment, although the speed we send to UR5 is smooth, the actual movement speed of UR5 is still jitter under the control of UR5 internal controller. In addition, the actual velocity of UR5 tool center point (TCP) is concentrated in the low-frequency and high-frequency parts of the spectrum as seen in Fig.6. The high-frequency part may be caused by gravity compensation, friction, motor noise, etc. As shown in Fig.7, we move joystick randomly in the workspace of the master, and record the filtered speed sent to UR5 and the actual filtered speed of UR5. The result shows that the trend of the speed curve of the slave is as basically same as that of master. The speed of the slave is lower than that of master because we send the discrete speed value and UR5 actually needs to speed up to the set value. If the value is too big, UR5 cannot reach the ideal value under the condition of 100 Hz position control frequency. In condition, due to gravity compensation, friction, motor noise and other potential factors, the actual speed of UR5 may be higher than the sent speed because we can't completely filter out irrelevant signal.

A Model 040GSE phantom from CIRS was used in ultrasound experiments and ultrasound gel was applied before

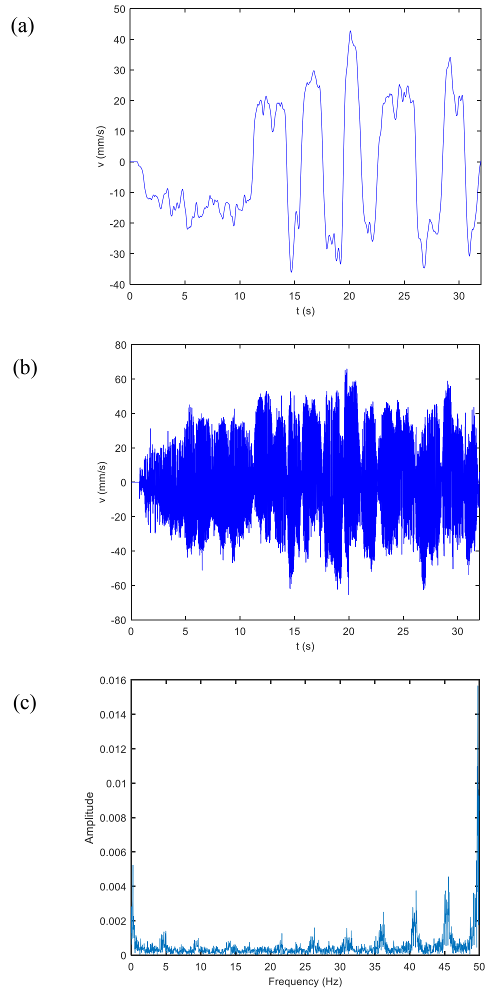

Fig. 6. (a) The filted speed of the Touch in the y-axis of the slave base coordinate (b) UR5 Tcp actual speed in z axis, (c) Spectrum of (b)

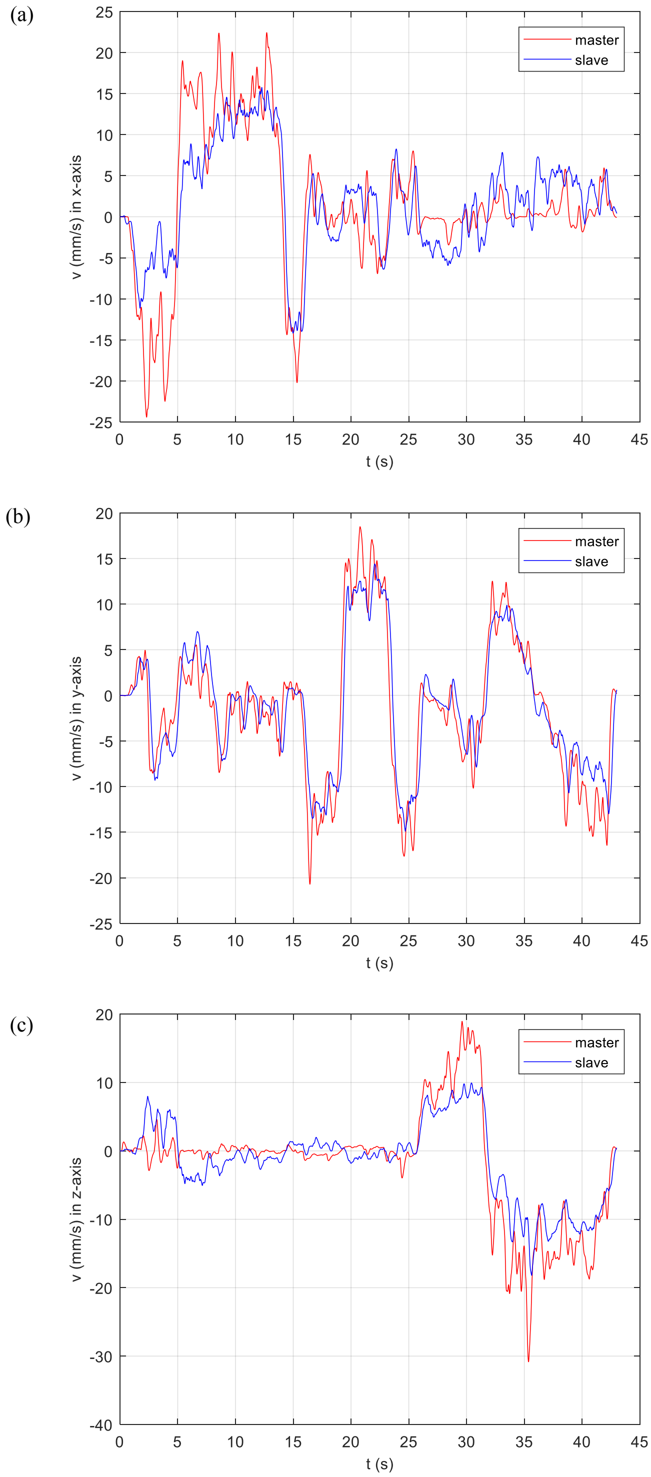

Fig. 7. Comparision of master and slave speed in slave base coordinate: (a) in slave x-axis, (b) in slave y-axis and (c) in slave z-axis

the experiments. Due to the lack of force sensor, ultrasound imaging of the phantom can only rely on the eyes and images to judge the contact between the ultrasonic probe and the phantom without force feedback. Without the force sensor, this experiment cannot fully prove that the proposed system can work well in robot-assisted ultrasound, but in the aspect of motion control, it can prove the feasibility of the ultrasound imaging.

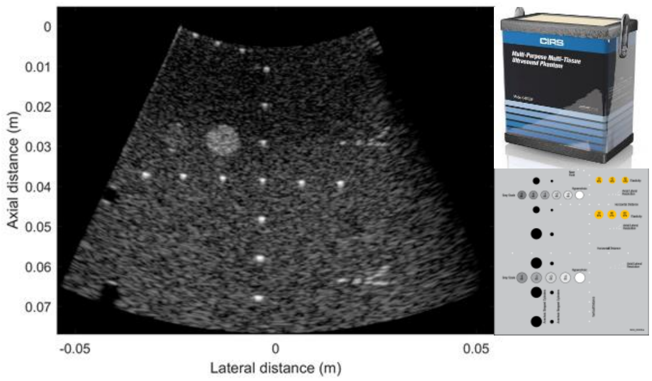

Fig. 8. Ultrasonic experimental image, phantom and specification of phantom

IV. CONCLUSIONS

In this paper, we develop a robot assisted ultrasound imaging system and propose a master-slave mapping relationship based on velocity control of incremental position and orientation. Experiments verify the effectiveness of master-slave speed tracking and the feasibility of ultrasound imaging. Our work lays the foundation for the remote ultrasound imaging system. Future research work will include enhancing the system real-time performance and improving the imaging efficiency by adding a force/torque sensor to the system.

ACKNOWLEDGMENT

This work was supported by Ltd. Wuhan United Imaging Healthcare Surgical Technology Co., Ltd.

REFERENCES

[1] Montaldo, G., Tanter, M., Bercoff, J., Benech, N., & Fink, M. Coherent plane-wave compounding for very high frame rate ultrasonography and transient elastography. IEEE transactions on ultrasonics, ferroelectrics, and frequency control, 56(3), pp.489-506, 2009.

[2] Guan, X., Wu, H., Hou, X., Teng, Q., Wei, S., Jiang, T & Xiong, L, Study of a 6DOF robot assisted ultrasound scanning system and its simulated control handle. In 2017 IEEE International Conference on Cybernetics and Intelligent Systems (CIS) and IEEE Conference on Robotics, Automation and Mechatronics (RAM), pp. 469-474, 2007.

[3] Barros-Gomes, S., Orme, N., Nhola, L. F., Scott, C., Helfinstine, K., Pislaru, S. V & Pellikka, P. A. Characteristics and Consequences of Work-Related Musculoskeletal Pain among Cardiac Sonographers Compared with Peer Employees: A Multiside Cross-Sectional Study. Journal of the American Society of Echocardiography, 2019.

[4] Monfaredi, R., Wilson, E., Azizi koutenaei, B., Labrecque, B., Leroy, K., Goldie, J & Cleary, K. Robot-assisted ultrasound imaging: Overview and development of a parallel telerobotic system. Minimally Invasive Therapy & Allied Technologies, 24(1), 54-62, 2015.

[5] Swerdlow, D. R., Cleary, K., Wilson, E., Azizi-Koutenaei, B., & Monfaredi, R. Robotic arm–assisted sonography: Review of technical developments and potential clinical applications. American Journal of Roentgenology, 208(4), 733-738, 2017.

[6] Meng, B., & Liu, J. (2015, June). Robotic ultrasound scanning for deep venous thrombosis detection using RGB-D sensor. In 2015 IEEE International Conference on Cyber Technology in Automation, Control, and Intelligent Systems (CYBER), pp. 482-486, 2015.

[7] Huang, Q., Lan, J., & Li, X. Robotic arm based automatic ultrasound scanning for three-dimensional imaging. IEEE Transactions on Industrial Informatics, 15(2), 1173-1182, 2018.

[8] Toporek, G., Wang, H., Balicki, M., & Xie, H. Autonomous image-based ultrasound probe positioning via deep learning (No. 119). EasyChair, 2018.

[9] Seo, J., Cho, J., Woo, H., & Lee, Y. Development of prototype system for robot-assisted ultrasound diagnosis. In 2015 15th International Conference on Control, Automation and Systems (ICCAS), pp. 1285-1288, 2015.

[10] Fjellin, J. E. Design of a Bilateral Master-Slave System with Haptic Feedback for Ultrasound Examinations. Master's thesis, Oslo, Norway: University of Oslo, 2013.

[11] Ju, Z. , Yang, C. , Li, Z. , Cheng, L. , & Ma, H. IEEE 2014 international conference on multisensor fusion and information integration for intelligent systems (mfi), teleoperation of humanoid baxter robot using haptic feedback. 1-6, 2014.

[12] Mathiassen, K., Fjellin, J. E., Glette, K., Hol, P. K., & Elle, O. J. An ultrasound robotic system using the commercial robot UR5. Frontiers in Robotics and AI, 3(1), 2016.

[13] Denavit, J. A kinematic notation for lower-pair mechanisms based on matrices. Trans. of the ASME. Journal of Applied Mechanics, 22, 1955.

[14] Zareinia, K., Maddahi, Y., Ng, C., Sepehri, N., & Sutherland, G. R. Performance evaluation of haptic hand-controllers in a robot-assisted surgical system. The International Journal of Medical Robotics and Computer Assisted Surgery, 11(4), 486-501, 2015.

[15] Sansanayuth, T., Nilkhamhang, I., & Tungpimolrat, K. Teleoperation with inverse dynamics control for phantom omni haptic device. In 2012 Proceedings of SICE Annual Conference (SICE) , pp. 2121-2126, 2012.

[16] Zandsteeg, C. J., Bruijnen, D. J. H., & Van de Molengraft, M. J. G.. Haptic tele-operation system control design for the ultrasound task: A loop-shaping approach. Mechatronics, 20(7), pp.767-777, 2010